Modified Thermal-Optical Analysis Using Spectral Absorption Selectivity to Distinguish Black Carbon from Pyrolized Organic Carbon

Odelle L. Hadley. Craig E. Corrigan. and Thomas W. Kirchstetter*

Scripps Institution of Oceanography, MC 0221, La Jolla, California 92093-0221 and Lawrence Berkeley National Laboratory, 1 Cyclotron Road, MS 70R0108B, Berkeley, California, 94720

Email: ohadley@ucsd.edu,

Tel: (858) 534-7757

Abstract

Black carbon (BC), a main component of combustion-generated soot, is a strong absorber of sunlight and contributes to climate change. Measurement methods for BC are uncertain, however. This study presents a method for analyzing the BC mass loading on a quartz fiber filter using a modified thermal-optical analysis method, wherein light transmitted through the sample is measured over a spectral region instead of at a single wavelength as the sample is heated. Evolution of the spectral light transmission signal depends on the relative amounts of light-absorbing BC and char, the latter of which forms when organic carbon in the sample pyrolyzes during heating. Absorption selectivities of BC and char are found to be distinct and are used to apportion the amount of light attenuated by each component in the sample. Light attenuation is converted to mass concentration based on derived mass attenuation efficiencies (MAE) of BC and char. The fraction of attenuation due to each component are scaled by their individual MAE values and added together as the total mass of light absorbing carbon (LAC). An iterative algorithm is used to find the MAE values for both BC and char that provide the best fit to the carbon mass remaining on the filter (derived from direct measurements of thermally evolved CO_2) at temperatures higher than 480°C. This method was applied to measure the BC concentration in precipitation samples collected from coastal and mountain sites in Northern California. The uncertainty in measured BC concentration of samples that contained a high concentration of organics susceptible to char ranged from 12 to 100 percent, depending on the mass loading of BC on the filter. The lower detection limit for this method was approximately 0.35 μg BC and uncertainty approached 20 percent for BC mass loading greater than 1.0 μg BC.

Keywords: black carbon, thermal-optical analysis, TOA, aerosol, air pollution

Introduction

Analysis of atmospheric aerosol pollution is integral to achieving a better understanding of anthropogenic influence on global and regional climate change (1). Aerosols and their associated feedbacks introduce some of the largest uncertainties facing climate forecasters today (2). Black carbon (BC), a main component of soot, represents one of the largest sources of uncertainty in quantifying the net effect of aerosols on climate (2-4). A large fraction of these uncertainties are due to the typically large errors associated with various BC measurement techniques. This study presents a modification to a thermo-optical analysis (TOA) method that is often used to quantify BC collected on filters, but is also subject to significant artifacts from organics present in the sample that pyrolize or char during thermal analysis. The distinctive spectral absorption properties of BC and these charred organics were used to distinguish the BC mass on the filter. This analysis method was developed specifically to analyze filtered precipitation samples, where the charred organic mass dominated the BC signal during TOA. This method is useful for any BC samples where pyrolysis of organics is a problem.

The most commonly used methods for measuring atmospheric BC concentration involve optical or a combination of thermal and optical characterization of aerosol samples collected on filters. These methods are imperfect, in part due to the non-standardized definition of BC. Method inter-comparisons, for example, yield BC estimates that can differ by as much as a factor of 7 (5,6). A brief description of BC measurement strategies is included below, although detailed reviews of techniques used to measure BC in aerosols may be found elsewhere (7,8).

Filter-based optical methods determine the mass of BC on the filter from measured light absorption, or attenuation, using a modification of the Beer-Lambert law (9):

$$BC = \frac{ATN * A}{MAE} \quad (1)$$

In this application concentration times path length is redefined as mass of BC on the filter divided by the sample area on the filter (A). Molar absorptivity is converted to mass attenuation (absorption) efficiency (MAE) and has units of m^2g^{-1}. For filter based measurements attenuation rather than absorption is often used because actual light absorption is enhanced due to multiple scattering by the filter (7).

Experimentally determined values of MAE are influenced by several factors. The filter used to collect the BC particles can have the most significant impact. For example, a highly reflective quartz fiber filter, like that in the widely-used aethalometer (10), scatters light to the particles and enhances approximately two-fold the amount of light absorbed by BC compared to that absorbed by the same mass of BC suspended in air (9,11). Thus, the distinction between the mass attenuation efficiency (MAE) of filter-bound BC and the mass specific *absorption cross-section* of atmospheric BC is important. Light-scattered away from the detector by non-absorbing particles can also lead to overestimation of the MAE (12), whereas the apparent MAE may decrease as the filter loading of BC increases (13). The size and mixing state of BC particles influence the MAE of both filter-bound and atmospheric particles (7,14,15). After applying corrections for filter-induced artifacts, the published range of MAE values for BC in air at 550 nm is 5 to 14 m^2g^{-1}, with a central value of 7.5+1.2 m^2g^{-1} (7,15). For BC on a quartz fiber filter, an enhancement factor of 2 yields a range of MAE values of approximately 10 to 20 m^2g^{-1}.

The thermal-optical analysis (TOA) of carbonaceous particles provides a measure of the total carbon (TC) in the sample and an estimate of how much is organic carbon (OC) versus elemental carbon (EC) (8). In most TOA methods, the sample is heated sequentially in inert (He) and oxidative (He/O_2 mixture) atmospheres, respectively, to volatilize and combust the sample carbon. Evolved carbonaceous material is oxidized to CO_2 or reduced to methane and quantified. Nominally, the carbon evolved during heating in the inert atmosphere is OC whereas the carbon evolved during heating in the oxidative atmosphere is EC. The challenge in TOA lies in differentiating the OC and EC. Early combustion of EC in the inert-phase and the formation of char (EC-like material that is refractory and light-absorbing) due to pyrolysis of OC can lead to large errors in the estimation of EC. Optical characterization of the sample either by measured transmission or reflectance of laser light is intended to monitor and correct for these sources of error. Several variations of TOA exist (8,16,17), including the one employed in this study (14). In this TOA method, the sample is heated in O_2 only (i.e, there is no inert phase) and light-transmission is used to distinguish between OC and BC. The light-absorbing, refractory carbon is referred to as BC instead of EC because optical absorbance, rather than the oxidative potential of the air in the sample chamber, is the primary indicator of carbon type. A new variation on the TOA method is the optical characterization of the sample over a broad spectral region, as opposed to at a single wavelength, in an attempt to improve the distinction between OC and BC.

Experimental section

Modifications were made to an existing TOA method for the purpose of determining BC content on Tissuequartz fiber filters. The BC was filtered from samples of rain and snow

water collected in various locations in Northern California. Sample water was passed through a series of three filters to ensure efficient BC retrieval from the filtrate. The filtration efficiency, tested prior to the analysis with laboratory standards of known quantities of soot in purified water, was 92+/-7%. High OC concentrations in the precipitation samples caused significant char formation on the filters during analysis and interfered with the determination of BC mass. The TOA method used in this study included broadband optical characterization of samples as they were heated. Differences in the spectral properties between BC and organic char were used to separate the absorption due to BC from that due to the char. Light transmission, from a white light emitting diode, over a spectral range of 400 to 900 nm wavelengths was measured with an Ocean Optics (model S2000) spectrometer. For this analysis, optical properties of the sample laden filter, combined with direct measurements of thermally evolved carbon, are used to determine the BC mass on the filter. This is the first use of spectral transmission data in estimating the BC content of samples.

Thermo-Optical Analysis

The carbon mass (C_{mass}) removed from the filter as a function of temperature increase was computed directly by summing the concentrations of evolved carbon atoms, calculated from measured moles of CO_2 per mole of O_2 (calculated from the oxygen carrier gas flow rate (0.2 L min^{-1})) and the sample temperature ramp rate (40º min^{-1}). The equation used to calculate C_{mass} is given in the supporting information. The sampling interval was 1^{o}C over the analysis range 50ºC to 700ºC) (13). Plotting TC as a function of temperature yields the carbon thermogram (Figures 1 & 2, solid line). The peaks correspond to different forms of carbon evolving at different temperatures. Prior work suggests that most OC evolves

between 50ºC and 450ºC, while BC generally evolves at temperatures between 400ºC and 700ºC (18). Estimating BC and OC solely on the basis of evolution temperature, however, is error-prone because the char formed from pyrolyzed OC may co-evolve with the BC. In addition, BC may combust at lower temperatures if catalytic materials are present in the sample (18,19), thereby shifting the BC further into the region of the thermogram dominated by the OC.

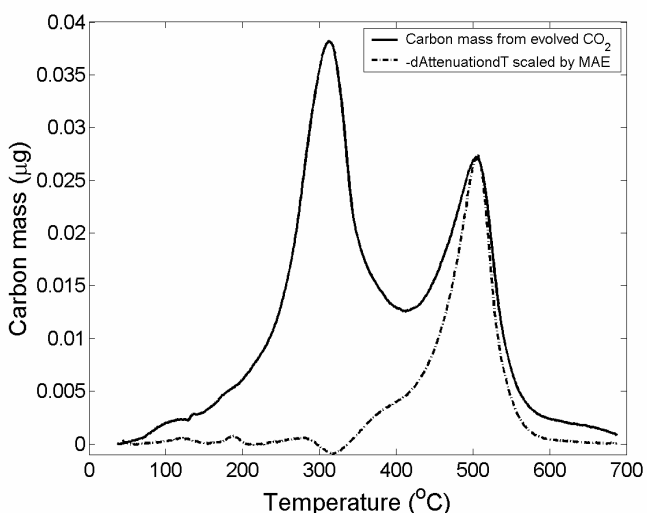

Figure 1. From laboratory standard, soot peak with organics. Change in attenuation is scaled to match the carbon (soot) peak at 500ºC.

Simultaneously measured changes in light attenuation (ATN) by the filter indicate the addition or removal of optically active carbon. $ATN(T)$ is determined from the transmittance of light through the filter as:

$$ATN(T) = -\ln\left[\frac{I_s(T)}{I_o} * \frac{I_o}{I_r}\right] \quad (2)$$

(9,14), where I_o is the intensity of light incident on the filter, $I_s(T)$ is the intensity of light measured on the other side of the loaded filter and is a function of temperature as light absorbing carbon is added and removed from the filter. I_r is the light intensity measured at T=700ºC, when all light absorbing carbon has been removed from the filter. A plot of the variation in ATN (i.e, the derivative of ATN with respect to temperature) versus temperature yields the optical thermogram (Figures 1 & 2, dashed line). When char formation is minimal and the sample does not darken during analysis (as evidenced by little or no decrease below baseline in the optical thermogram), the black carbon and ATN thermogram peaks overlap (Figure 1) and the optical thermogram can be used to estimate the BC content of the sample. Figure 1 shows carbon and optical thermograms for a sample of particles generated with the laboratory diffusion flame (13), where the optical thermogram is scaled to the height of the carbon thermogram. The scaling factor is the MAE of the BC and it varies with sample.

For many atmospheric samples, the left side of the BC thermogram peak may be obscured by co-evolving carbonaceous material, such as refractory organics or char formed by pyrolysis of organics during analysis (Figure 2). When this occurs, it is unclear which region of the carbon thermogram to integrate for BC mass. Integrating the carbon thermogram after the attenuation (that initially increased due to charring organics) returns to its original value over-estimates the amount of BC in the sample. This is because a small amount of BC may evolve before attenuation returns to its initial value. As the measured MAE for char was typically much smaller than the MAE than BC, the BC removal will have a much greater affect on reducing attenuation than the same amount of char. After attenuation returns to initial values, a significant mass of char still residing on the filter will

be interpreted as BC in the thermogram. Spectral-optical characterization of the sample can be used to aid in the distinction between BC and co-evolving char, as described below.

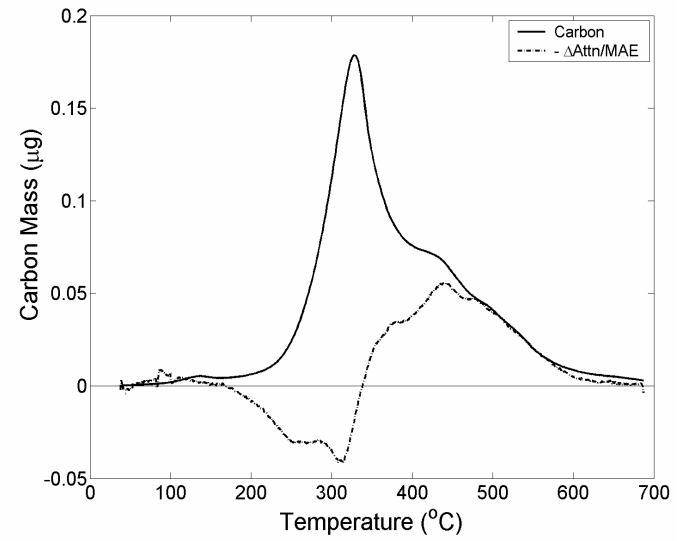

Figure 2. From field sample of snow melt water. Change in attenuation is multiplied by -1 and scaled to match carbon mass. The scaling factor is the MAE of both the charred OC and the BC. Charred OC obscures the BC signal.

Separating Pyrolyzed (charred) Organic Carbon from Black Carbon

The dependence of absorption, or in this case, attenuation, on wavelengths, λ, is often expressed as a power law (14,20):

$$ATN(\lambda) = c\lambda^{-k} \quad (3)$$

where k is the absorption angstrom exponent (AAE) and c is the attenuation coefficient. Differences in the AAE values for pure BC, pure char and the mixture of BC and char allowed the relative contributions of BC and char to the light attenuation on the filter to be

determined throughout thermal processing. Direct measurements of thermally evolved CO_2 were used to determine the MAE for both BC and char, as well as provide the uncertainty in the calculated mass of BC. A more complete description of the process and subsequent error analysis follows.

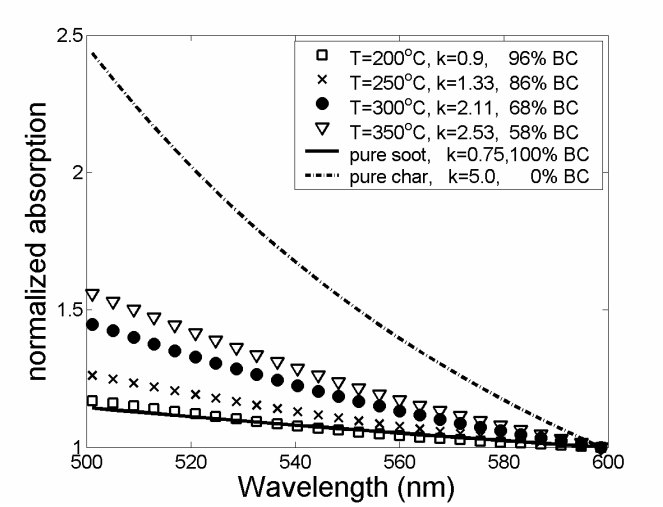

Figure 3. Spectral dependence of light absorption by soot and by char. The angstrom exponent, k, describes change in absorption as a function of wavelength (abs = λ^{-k}). Absorption is normalized to 600 nm. T refers to temperature.

The transmitted intensity of light ($500<\lambda<600$ nm) through a sample filter was continuously monitored throughout thermal evolution. This spectral region was not extended to longer or shorter wavelengths due to insufficient LED output below 480 nm and contamination of the light signal from the furnace heat at wavelengths greater than 600 nm for temperatures greater than 500ºC. Char typically began forming at T=200ºC. As the amount of char increased on the filter, light attenuation also increased (Figure 2), as did the

spectral dependence of absorption or measured AAE value (Figure 3). The total amount of light attenuated by the char and BC on the filter may be approximated as the sum of the attenuation due to the pure BC and that due to the char. Thus equation 3 may be rewritten as:

$$ATN(\lambda,T) = c_1(T)\lambda^{-k_{BC}} + c_2(T)\lambda^{-k_{char}} \approx c(T)\lambda^{-k_m}, \text{ for } 500\text{nm} \le \lambda \le 600\text{nm} \quad (4)$$

As the sum of two exponentials does not follow a simple power law, equation 4 is an approximation that is valid only over the specified region of the spectrum as shown by the shaded gray area in Figure 4. $\mathbf{k_{BC}}$, $\mathbf{k_{char}}$, and $\mathbf{k_m}$ are respectively, the absorption angstrom exponents (AAE) of pure BC, pure char, and the measured LAC (light absorbing carbon), i.e. BC plus char on the filter. $\mathbf{k_{BC}}$, which is the AAE measured for laboratory soot between 500-600nm, was 0.75 +/- 0.02. The average AAE for BC in field samples was also 0.75, however the uncertainty was higher at +/-0.15. In equations 4 & 6, $\mathbf{k_{BC}}$ is the measured AAE of the sample prior to thermal processing. $\mathbf{k_{char}}$ was measured during TOA of the "back-up" filters from field sample filtration. These filters contained no BC, verified by optical measurements before and after TOA, and thus attenuation changes during thermal processing were due only to charring OC. $\mathbf{k_{char}}$ was 5+/-1. To determine the AAE value of the combined BC and char, or $\mathbf{k_m}$, linear regression is used to find the slope of the log of measured attenuation with respect to the log of wavelength between 500 and 600 nm and at each temperature (Equation 5).

$$k_m(T) = -\frac{\Delta \ln(ATN(\lambda,T))}{\Delta \ln(\lambda)} \quad (5)$$

The attenuation constant, c, which is solved for equation 4 once k_m is known, depends directly on the mass of light absorbing carbon on the filter and is therefore a function of

temperature. Finally, solutions for c1 and c2 may be determined using two different values of lamda near 550 nm (λ_1= 530 nm and λ_2 = 570 nm). Thus equation 4 can be made into two equations, and the two unknown constants (c_1 and c_2) may be solved for algebraically (see supporting information).

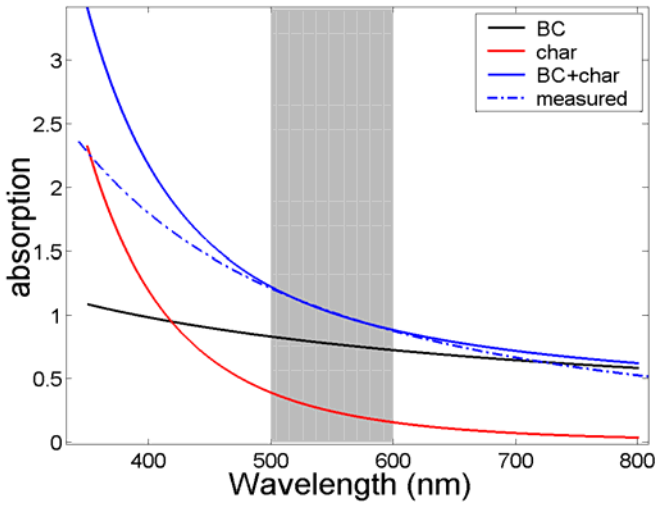

Figure 4. The black and red lines are the spectral absorption of pure BC and char respectively and follow the equation: abs = $\mathbf{A}\lambda^{-k}$, where k for BC is 0.75 and k for char is 5. **A** is determined uniquely for BC and char. The blue solid line is the summation of BC and char (red and black lines). The blue dashed line is created from the measured values for k and A between 500 and 600 nm (the shaded region).

Figure 4 illustrates how solutions for c_1 and c_2 are applicable over the specified spectral region, but under-predict the absorption at shorter wavelengths. This phenomenon has been previously observed in field measurements of soot and organic carbon mixtures (14,20).

These equations further imply that derived AAE values for field samples, which would typically be a mix of absorbers, are valid only over the spectral region measured and extrapolating absorption at longer or shorter wavelengths may not be appropriate. The fraction of attenuation change at 550 nm due to BC (**a**) and that due to char (1-**a**) at each temperature during thermal optical analysis, was calculated from equation 4 as:

$$a(\lambda_{550nm}, T) = \frac{c_1(T)\lambda_{550nm}^{-k_{BC}}}{c(T)\lambda_{550nm}^{-k_m}} \quad (6)$$

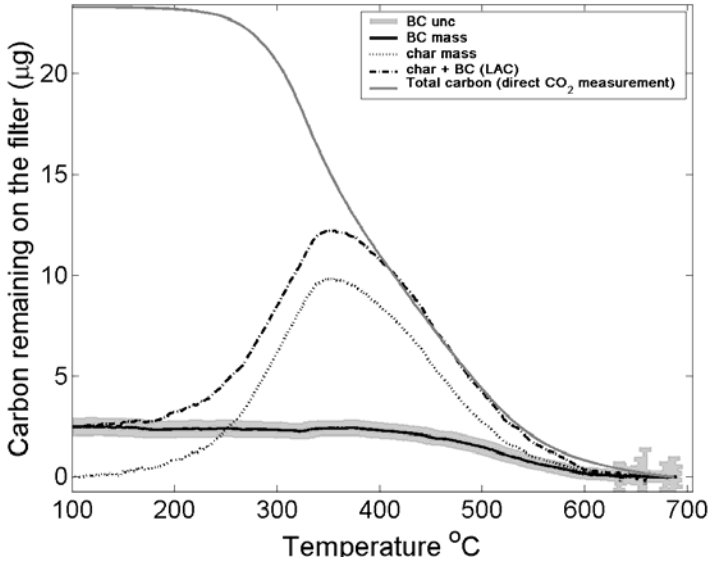

Figure 5. BC and char contribution to total light absorbing carbon. Total carbon is the total amount of carbon remaining on the filter and was derived from the direct measurement of evolved CO_2 as a function of temperature.

Assuming that all of the carbon evolved at temperatures greater than 480ºC was absorbing and comprised of the original BC and the char, MAE values for BC and char were determined using a best fit to the direct carbon measurement at temperatures greater

than 480ºC. An iterative routine was used to find MAE_{BC} and MAE_{char}, such that when the BC and char attenuation components were individually scaled by these values and summed, the reconstructed curve matched the direct measurement of carbon mass remaining on the filter at temperatures greater than 480ºC (Figure 5). The equation for calculating carbon mass remaining on the filter as a function of temperature is given in the supporting information.

The range of previously published MAE values for BC on quartz fiber filters constrained the values for MAE_{BC} between 10 and 20 m^2/g. The range of values for MAE_{char}, 0.5 to 7 m^2/g, was found using the same field sample back-up filters used to find $\mathbf{k_{char}}$. The fitting algorithm cycled through the range of MAE values at increasing increments of 0.05 m^2g^{-1} and found those values corresponding to the minimum RMS (root mean square) difference between the measured carbon mass and the reconstructed sum of BC and char mass. BC mass remaining on the filter during TOA was determined by combining the Beer-Lambert law as shown in equation 1 with the derived fraction of attenuation due to BC calculated using equation 6 and the MAE_{BC} value corresponding to the best fit with the directly measured carbon mass.

$$BC(T) = \frac{a_{550nm}(T) * ATN_{550nm}(T) * A}{MAE_{BC}} \quad (7)$$

Results and Discussion

The average calculated mass attenuation efficiency for the BC filtered from 29 precipitation samples was 13.97 +/- 4.2 m^2g^{-1}. This wide range of MAE values is likely due to variability in source, chemical structure, and size of the BC particles. Absorption enhancement due to coating of the BC particles by sulfates and organics (15) would not

apply here as the water soluble coating should be removed by the water sample. This may also explain why the MAE values tend to be on the lower end of published values for BC MAE. The average calculated MAE of char was 3.1 +/- 2.3 m^2g^{-1}.

A root mean square (RMS) difference was calculated from the closeness of the fit between the reconstructed LAC (BC plus char) mass and the direct measurement of total carbon mass from evolved CO_2 at temperatures greater than 480ºC. The RMS difference, which represents the uncertainty in BC mass, was assumed to be entirely due to the uncertainty in the MAE_{BC}, as opposed to uncertainties in the carbon measurement or the MAE of char. The uncertainty in the MAE_{BC} for each sample can be expressed as a simple calculation:

$$\sigma_{MAE_{BC}} = \left| \frac{dMAE_{BC}}{dBC} \right| * RMS \qquad (8)$$

The uncertainty in **a**, calculated from the uncertainties in the derived values for $\mathbf{k_{BC}}$, $\mathbf{k_{char}}$, and $\mathbf{k_m}$, along with the uncertainty in measured attenuation (+3) and MAE_{BC} are propagated through equation 7 and give an uncertainty of BC mass at each temperature. The overall uncertainty in the final calculation for BC mass is the sum of the standard deviation from the retrieved BC mass between T=100ºC and T=300ºC and the average calculated uncertainty over the same temperature range. Figure 6 shows the percent uncertainty plotted as a function of total BC mass on the filter. The lower detection limit for this method is approximately 0.35 μg of BC. For BC mass greater than 1.0 μg, the percent uncertainty approaches 20%. The overall uncertainty is unique for each sample and ranges from 12% to 100%, depending on BC concentration, char, and dust content.

During thermal processing, some inorganic material may still contribute to changes in the light transmission. For example, oxidation of metals in the dust, such as Fe(II) to Fe(III),

may affect light absorption measurements at visible wavelengths, however the MAE of dust is a factor of one hundred less than the MAE of BC (21). Consequently the signal interference of oxidizing metals on BC should be negligible in most field samples. If the field sample does contain a high enough concentration of metals relative to the BC concentration, the oxidation of these metals at high temperatures could significantly increase the absorption of visible wavelengths at temperatures greater than 500°C and contaminate the reference transmission, as well as obscure the AAE measurements. This effect was observed to varying degrees in a few of the field samples used in this study, which were subsequently removed from this analysis. Comparing the transmission measurement of a dust laden sample prior to and after thermal processing, revealed that enhanced absorption in the visible wavelengths did not extend past 800 nm. Thus, for cases where dust contamination is severe, the change in attenuation at 880 nm may still be used to estimate BC mass using the optical method alone.

Although there is still significant error associated with the BC measurements, this new BC analysis method provides a way to separate the BC signal from the charring signal of organics, a significant source of error in TOA of precipitation filtrate. Furthermore, errors less than 20% are at the lower end for previously published uncertainties in BC mass measured in snow and rain water, between 30% and 50% (8,22,23). This approach also provides a way to characterize measurement dependent uncertainties for each discrete sample, rather than assigning an uncertainty estimate to an entire analytical procedure. The MAE used for BC and for char result in mass calculations, that when summed, are consistent with the direct measure of total carbon mass obtained from the thermo-optical analyzer.

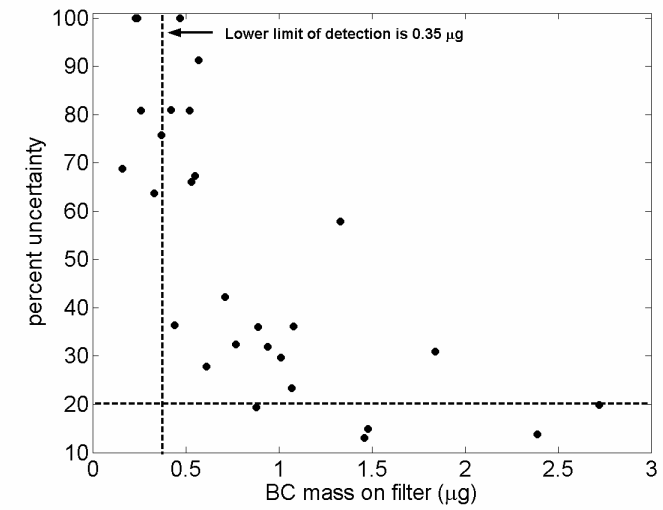

Figure 6. Percent uncertainty for field samples, vs filter loading. Dashed lines indicates that uncertainty approaches a constant value of 20% for BC mass above 1.0 μg and that the lower limit of detection is 0.35 μg of BC.

Relative to TOA of BC in atmospheric aerosols, the charring of organics from precipitation samples presented much higher signal interference in both the thermally dependent direct measurement of carbon and the optically inferred calculation. An analysis of light attenuation over a specific spectral region, rather than at a single wavelength, has led to a method for separating BC mass from organic char using individual absorption angstrom exponent values. Applying direct carbon measurements from evolved CO_2 helped constrain and validate the MAE values obtained and used to find the BC concentration for each individual sample.

The techniques described above may also be applied to measurements of BC in ambient aerosol analysis. Further development of this method may allow for determining relative source contributions to BC aerosol from biomass burning and urban processes. Previous

work has shown that the spectral dependence of absorption by BC particles generated by these processes differ similarly to BC and char. Soot generated from fossil fuel burning and urban processes have AAE values very close to that of the pure laboratory BC, while biomass burning produces soot containing spectral characteristics analogous to that of the char (14,20). Careful examination of the AAE values for soot generated by varying methods could potentially allow more accurate source apportionment for light absorbing aerosol.

Acknowledgments

We thank Guido Franco and the California Energy Commission for their support (CEC Award #MR-06-01B). We also thank Prof. T. Novakov and Jefferey Aguiar for advice and assistance during the laboratory phase of this study.

References

(1) Penner, J. E.; Andreae, M.; Annegarn, H.; Barrie, L.; Feichter, J.; Hegg, D.; Jayaraman, A.; Leaitch, R.; Murphy, D.; Nganga, J.; Pitari, G. Aerosols, their Direct and Indirect Effects. In *Climate Change 2001: The Scientific Basis. Contribution of Working Group I to the Third Assessment Report of the Intergovernmental Panel on Climate Change*; Houghton, J. T., Ding, Y., Griggs, D. J., Noguer, M., Linden, P. J. v. d., Dai, X., Maskell, K., Johnson, C. A., Eds.; Cambridge University Press: Cambridge, United Kingdom and New York, NY, USA, 2001; pp 289 - 348.

(2) Ramaswamy, V.; Boucher, O.; Haigh, J.; Hauglustaine, D.; Haywood, J.; Myhre, G.; Nakajima, T.; Shi, G. Y.; Solomon, S. Radiative Forcing of Climate Change. In *Climate Change 2001: The Scientific Basis. Contribution of Working Group I to the Third Assessment Report of the Intergovernmental Panel on Climate Change*; Houghton, J. T., Ding, Y., Griggs, D. J., Noguer, M., Linden, P. J. v. d., Dai, X., Maskell, K., Johnson, C. A., Eds.; Cambridge University Press: Cambridge, United Kingdom and New York, NY, USA, 2001; pp 351 - 416.

(3) Jacobson, M. Z. *Nature* **2001**, *409*, 695-697.

(4) Penner, J. E.; Zhang, S. Y.; Chuang, C. C. *J Geophys Res-Atmos* **2003**, *108*, 4657, doi:4610.1029/2003JD003409.

(5) Watson, J. G.; Chow, J.; Chen, L. W. A. *Aerosol and Air Quality Research* **2005**, *5*, 65-102.

(6) Currie, L. A.; Benner, B. A.; Kessler, J. D.; Klinedinst, D. B.; Klouda, G. A.; Marolf, J. V.; Slater, J. F.; Wise, S. A.; Cachier, H.; Cary, R.; Chow, J. C.; Watson, J.; Druffel, E. R. M.; Masiello, C. A.; Eglinton, T. I.; Pearson, A.; Reddy, C. M.; Gustafsson, O.; Quinn, J. G.; Hartmann, P. C.; Hedges, J. I.; Prentice, K. M.; Kirchstetter, T. W.; Novakov, T.; Puxbaum, H.; Schmid, H. *J Res Natl Inst Stan* **2002**, *107*, 279-298.

(7) Bond, T. C.; Bergstrom, R. W. *Aerosol Sci Tech* **2006**, *40*, 27-67.

(8) Chow, J. C.; Watson, J. G.; Chen, L. W. A.; Arnott, W. P.; Moosmuller, H. *Environ Sci Technol* **2004**, *38*, 4414-4422.

(9) Weingartner, E.; Saathoff, H.; Schnaiter, M.; Streit, N.; Bitnar, B.; Baltensperger, U. *J Aerosol Sci* **2003**, *34*, 1445-1463.

(10) Hansen, A. D. A. *The Aethalometer*; Magee Scientific Company: Berkely CA, 2003.

(11) Bodhaine, B. A. *J Geophys Res-Atmos* **1995**, *100*, 8967-8975.

(12) Arnott, W. P.; Hamasha, K.; Moosmuller, H.; Sheridan, P. J.; Ogren, J. A. *Aerosol Sci Tech* **2005**, *39*, 17-29.

(13) Kirchstetter, T. W.; Novakov, T. *Atmos Environ* **2007**, *41*, 1874-1888.

(14) Kirchstetter, T. W.; Novakov, T.; Hobbs, P. V. *J Geophys Res-Atmos* **2004**, *109*, D21208, doi:21210.21029/22004JD004999.

(15) Liousse, C.; Cachier, H.; Jennings, S. G. *Atmos Environ a-Gen* **1993**, *27*, 1203-1211.

(16) Lavanchy, V. M. H.; Gaggeler, H. W.; Nyeki, S.; Baltensperger, U. *Atmos Environ* **1999**, *33*, 2759-2769.

(17) Petzold, A.; Niessner, R. *Mikrochim Acta* **1995**, *117*, 215-237.

(18) Novakov, T.; Corrigan, C. E. *Mikrochim Acta* **1995**, *119*, 157-166.

(19) Mikhailov, E. F.; Vlasenko, S. S.; Podgorny, I. A.; Ramanathan, V.; Corrigan, C. E. *J Geophys Res-Atmos* **2006**, *111*, (D7), D07209 doi:07210.01029/02005JD006389.
(20) Bergstrom, R. W.; Pilewskie, P.; Russell, P. B.; Redemann, J.; Bond, T. C.; Quinn, P. K.; Sierau, B. *Atmos Chem Phys* **2007**, *Discuss., 7*, 10669-10686.
(21) Clarke, A. D.; Shinozuka, Y.; Kapustin, V. N.; Howell, S.; Huebert, B.; Doherty, S.; Anderson, T.; Covert, D.; Anderson, J.; Hua, X.; Moore, K. G.; McNaughton, C.; Carmichael, G.; Weber, R. *J Geophys Res-Atmos* **2004**, *109*, D15S09, doi:10.1029/2003JD004378.
(22) Chow, J. C.; Watson, J. G.; Crow, D.; Lowenthal, D. H.; Merrifield, T. *Aerosol Sci Tech* **2001**, *34*, 23-34.
(23) Clarke, A. D.; Noone, K. J. *Atmos Environ* **1985**, *19*, 2045-2053.